Constructal pattern of solar chimney power plants on land

Atit Koonsrisuk[*1], Sylvie Lorente[2] and Adrian Bejan[3]

[1] Suranaree University of Technology, School of Mechanical Engineering, Institute of Engineering, Muang District, Nakhon Ratchasima 30000, Thailand

[2] Université de Toulouse ; UPS, INSA ; LMDC (Laboratoire Materiaux et Durabilite des Constructions) ; 135, avenue de Rangueil ; F-31 077 Toulouse Cedex 04, France

[3] Duke University, Department of Mechanical Engineering and Materials Science, Durham, North Carolina 27708-0300, USA

* Corresponding Author: Tel: 044 224 515, Fax: 044 224 613,

E-mail: atit@sut.ac.th

Abstract

In this article we show how to use constructal design to distribute solar chimney power production on available land area most efficiently. We find that the power generated per unit of land area is proportional to the length scale of the power plant. Because of the flow resistances associated with distributing the power over a territory, the size of the territory must be finite and optimally allocated to each power plant. Several patterns of the multi-scale plants on a square area are explored. The global performance of such patterns is greater when more land area is allocated to the largest plant. It was found that this performance depends comparatively less on the total land area covered by all power plants.

Keywords*:* solar chimney; solar tower; constructal, distributed energy systems; multi-scale power plants.

1. Introduction

The solar chimney is a power plant that uses (1) solar radiation to raise the temperature of the air, and (2) buoyancy to accelerate the air flowing through the system. The main features of the solar chimney are sketched in Fig. 1. Air is heated as a result of the greenhouse effect under a transparent roof (the collector). Because the roof is open around its periphery, the buoyancy of the heated air draws a continuous flow from the roof perimeter into the chimney. A turbine is set in the path of the air current to convert partially the useful energy of the flowing air into electricity.

The concept of solar chimney power plant was proposed initially by the group of engineers led by Prof. Jörg Schlaich [1]. Later, Pasumarthi and Sherif [2] developed an approximate mathematical model to study the effect of various environmental conditions and geometry on the temperature, velocity and power output of a solar chimney system, followed by a subsequent work [3] which validates the proposed model against experimental data from the demonstration

models built in Florida. In 1999, Padki and Sherif [4] conducted some of the earliest work on the thermo-fluid analysis of a solar chimney plant. Lodhi [5] presented a comprehensive analysis of the chimney effect, power production and efficiency and estimated the cost of the solar chimney power plant set up in developing nations. Numerical simulations were carried out by Pastohr et al. [6] to improve the description of the operation mode and efficiency by coupling all parts of the solar chimney power plant including the ground, collector, chimney, and turbine. Ming et al. [7] proposed a mathematical model in which the effects of various parameters such as the tower height and radius, collector radius and solar radiation, on the relative static pressure, driving force, power output and efficiency can be investigated. They also performed numerical simulations to analyze the characteristics of heat transfer and air flow in the system with an energy storage layer [8]. Kashiwa and Kashiwa [9] have proposed using of the solar chimney for extracting fresh water from the atmosphere. The idea is to use an expansion cyclone separator that would be placed at the base of the chimney for condensing and removing atmospheric water. In [10], the feasibility of solar chimney power plants as an environmentally acceptable energy source for small settlements and islands of countries in the Mediterranean region was presented. They concluded that building of solar chimney power plants in the Mediterranean region is only profitable over the long term, but not the short term. The concept of integrating a collector of the solar chimney with a mountain hollow is presented and described by Zhou et al. [11].

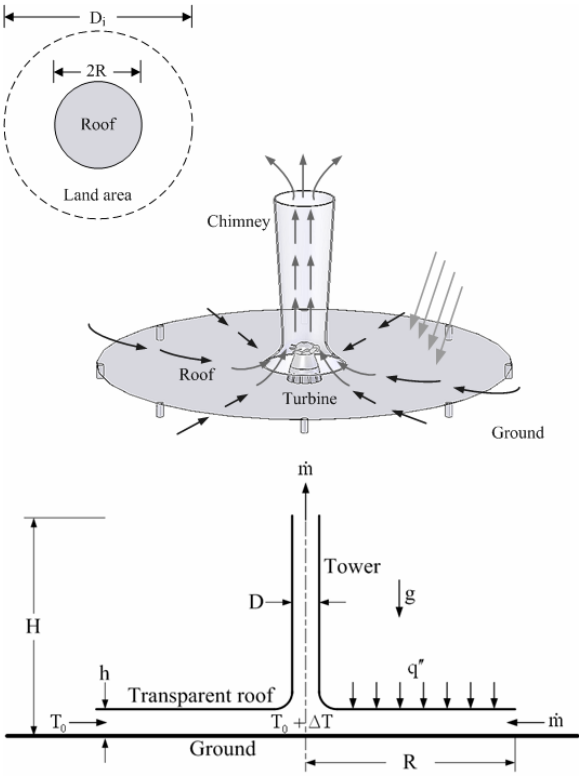

Figure 1

Several commercial solar chimney power plants have been proposed in the research literature. Solar chimneys with a 1000 m-diameter collector and 1000 m-high chimney were presented in Schlaich [1], as power plants with an electrical power capacity of hundreds of MW. A case study for the northwestern regions of China [12] concluded that the solar chimney power plant in which the height and diameter of the chimney are 200 m and 10 m, and the collector radius is 500 m should produce 110-190 kW of electric power. Bilgen and Rheault [13] proposed to construct a solar chimney on a sloped surface or on a suitable hill in a high latitude area. They showed analytically that a nominal power of 5 MW would be produced by a system with a collector area of 950,000 m^2 and an equivalent chimney height (= hill height + chimney height) of 547 m. A system with a 1500

m-high chimney was simulated by several authors [14-16]. Pretorius and Kröger [17] and Bernardes et al. [18] analyzed a plant that has a chimney with a height of 1,000 m, diameter of 210 m, and collector of radius of 5,000 m. It was clear that these plants would require a large investment in construction and operation. Consequently, any means of optimizing the design of the solar chimney power plant to reduce the capital outlay, while maintaining the average power production, would significantly increase the attractiveness of this renewable source of energy.

The work described in this paper is stimulated by the quest for better designs, and focuses on the generation of shape and structure by maximizing global performance of the flow system based on constructal theory [19]. We show that the configuration of the solar chimneys can be determined, along with the scaling rules for being able to distribute multi-scale power plants on a given territory.

The system geometry is simplified to that of a horizontal disc placed above the ground, with a vertical cylinder in the center of the disc. The solar chimney configuration has the four dimensions shown in Fig. 1: D, H, R and h. We assume that the flow is fully developed and turbulent in all the flow passages, and that the friction factors in the vertical tube (f_y) and the horizontal channel (f_x) are approximately constant. The air flow rate ($\dot{m}$) enters at atmospheric temperature (T_0) and is heated with uniform heat flux (q'') as it flows to the base of the chimney, where its temperature reaches $T_0 + \Delta T$. It is assumed that the solar radiation absorbed by the chimney is negligible with respect to the solar heat gain of the collector.

The air stream is driven by the buoyancy effect due to the vertical column of hot air (height H, temperature $T_0 + \Delta T$), which communicates with the ambient air of the same height and lower temperature (T_0). The net pressure difference that drives the air stream in the tower is [20]

$$\Delta P = \rho_{T_0} gH - \rho_{T_0+\Delta T} gH = \rho \beta gH \Delta T \qquad (1)$$

where ρ is the average air density, and β is the coefficient of volumetric thermal expansion.

The pumping effect (ΔP) is opposed by friction forces in the vertical tube (ΔP_y) and in the horizontal channel (ΔP_x) and the acceleration due to flow area reduction (ΔP_{acc}). For the vertical tube, the longitudinal force balance is

$$\Delta P_y \, \pi D^2/4 = \tau_w \pi DH \qquad \textbf{(2)}$$

where τ_w is the wall shear stress. The wall shear stress is expressed in terms of the friction factor f, which is defined as

$$\tau_w = f \frac{1}{2} \rho U^2 \qquad \textbf{(3)}$$

Combining Eqs. (2)-(3), we obtain

$$\Delta P_y = f_y \frac{4H}{D} \frac{1}{2} \rho U_y^2 \qquad \textbf{(4)}$$

where $U_y = \dot{m}/\left(\rho \pi D^2/4\right)$. The pressure loss along the horizontal channel (under the roof) is determined from the force balance

$$\Delta P_x \, 2\pi Rh = \tau_w 2\pi R^2 \qquad \textbf{(5)}$$

where $2\pi R^2$ is the area scale of the roof and ground contact surface in the horizontal channel. Consequently, the pressure loss in the horizontal passage is

$$\Delta P_x = f_x \frac{R}{h}\frac{1}{2}\rho U_x^2 \qquad (6)$$

where U_x is the average air speed at the entrance, $U_x = \dot{m}/(\rho 2\pi Rh)$. The horizontal flow experiences acceleration and heating in a channel with variable cross-sectional area A_c [21]

$$dP = \frac{\rho U^2}{(1-M^2)}\left(\frac{dA_c}{A_c} - \frac{q''dA_r}{\dot{m}c_pT}\right) \qquad (7)$$

Next we assume that in the horizontal flow the quantities q'', c_p, ρ and T are approximately constant. The Mach number, M, is negligible, and Eq. (7) reduces to

$$\Delta P_{acc} = \frac{\dot{m}^2}{2\rho_0}\left(\frac{1}{A_2^2} - \frac{1}{A_1^2}\right) - \frac{\dot{m}q''}{2\pi h^2 \rho_0 c_p T_0}\ln\frac{R}{D/2} \qquad (8)$$

where 1 and 2 denote the channel entrance and channel exit, respectively. Equation (8) shows that the pressure tends to increase due to heat addition (the second term) while it tends to decrease due to flow area reduction toward the roof center (the first term). An order of magnitude analysis reveals that the first term is much greater than the second term. In addition, because $A_1^2 >> A_2^2$, Eq. (8) becomes

$$\Delta P_{acc} \cong \frac{\dot{m}^2}{\rho_0 \pi^2 D^4/8} \qquad (9)$$

The losses balance the driving pressure difference, $\Delta P = \Delta P_y + \Delta P_x + \Delta P_{acc}$, therefore

$$\rho\beta\Delta T g H = f_y \frac{2H}{D}\rho\left(\frac{\dot{m}}{\rho\pi D^2/4}\right)^2 + f_x \frac{R}{2h}\rho\left(\frac{\dot{m}}{2\rho\pi Rh}\right)^2 + 2\rho\left(\frac{2\dot{m}}{\rho\pi D^2}\right)^2 \qquad (10)$$

Equation (10) relates the flow rate ($\dot{m}$) to the excess temperature reached at the base of the cylinder (ΔT). The second equation needed for determining $\dot{m}$ and ΔT uniquely is the first law of thermodynamics for the horizontal channel as a control volume:

$$q''\pi R^2 = \dot{m}c_p\Delta T \qquad (11)$$

We assume that D is considerably smaller than R (or that $A_1^2 >> A_2^2$), so that the area used by the solar collector is roughly πR^2, instead of $\pi[R^2 - (D/2)^2]$. By eliminating ΔT between Eqs. (10) and (11), we obtain

$$\dot{m}^3 = \frac{C_1 R^2 H}{\frac{C_2 H}{D^5} + \frac{C_3}{Rh^3} + \frac{1}{D^4}} \qquad (12)$$

where $C_{1,2,3}$ are three constants

$$C_1 = \frac{\rho^2\beta g q''\pi^3}{8c_p} \qquad (13)$$

$$C_2 = 4f_y \qquad (14)$$

$$C_3 = \frac{f_x}{64} \qquad (15)$$

The corresponding excess temperature at the base of the tower is

$$\Delta T = \frac{\pi q'' R^2}{\dot{m}c_p} \qquad (16)$$

3. Power versus size

The generation of power calls for a design that maximizes $\dot{m}$ and ΔP as a product. The thermodynamic ideal level of the power produced by a turbine inserted in a duct with the air stream $\dot{m}$ driven by the pressure difference ΔP is

$$\dot{W} \sim \dot{m}\Delta P/\rho \sim C_4 H R^2 \qquad (17)$$

where

$$C_4 = \frac{\beta g q''\pi}{c_p} \qquad (18)$$

One measure of the size of the power plant is the weight of the whole plant, which is

proportional to the total surface of the chimney and the roof,

$$A = \pi DH + \pi R^2 \qquad \textbf{(19)}$$

To maximize the $\dot{W}$ function (17) with respect to H and R, subject to constraint (19), is equivalent to seeking the extremum of the aggregate function formed by combining the right sides of Eqs. (17) and (19),

$$\Psi = C_4 HR^2 + \lambda\left(DH + R^2\right) \qquad \textbf{(20)}$$

Solving $\partial\Psi/\partial H = 0$ and $\partial\Psi/\partial R = 0$, and eliminating λ, we obtain the geometric scaling rule $H = R^2/D$, or

$$\frac{H}{R} = \frac{(A/2\pi)^{1/2}}{D} \qquad \textbf{(21)}$$

The maximized power level that corresponds to the optimal configuration is

$$\dot{W}_{max} = C_4 \frac{A^2}{4\pi^2 D} \qquad \textbf{(22)}$$

This result shows that the power level increases rapidly as the aggregate size increases. If $A^{1/2}$ represents the length scale of the entire flow system, then it is reasonable to anticipate that D will vary more or less in proportion with $A^{1/2}$. This leads to the conclusion that $\dot{W}_{max}$ scales with $A^{3/2}$, i.e. with the length scale cubed.

In addition, because R^2 scales with A [cf. Eq. (19)], it follows that the maximum power generated per land area $\left(\dot{W}_{max}/\pi R^2\right)$ varies in proportion with the length scale of the installation, $A^{1/2}$. The conclusion is that the maximum use of land surface requires the use of larger solar chimney power plants. The existence of "economies of scale" raises the question of how to extract most solar power from an available land area. This question applies to all proposals of power generation from distributed (low density) resources of energy. We return to this aspect in the concluding section.

4. Few large, or many small ?

Larger power plants produce more power per unit of territory, and this can be exploited for benefit on a large fixed territory that is to be covered completely with power plants. To begin with, the power produced per unit area $\left(\dot{W}/\pi R^2\right)$ is proportional to the energy conversion efficiency of the power plant,

$$\eta = \frac{\dot{W}}{q''\pi R^2} \qquad \textbf{(23)}$$

because the solar heat input per unit area $\left(q''\right)$ is a constant parameter of the region. The conclusion that η increases with the size of the installation $\left(R \text{ or } A^{1/2}\right)$ agrees qualitatively with observations of scaling in power plants and refrigeration plants of all sizes [22]. The larger installations are more efficient.

This scaling has two important implications in energy design for global sustainability. The reason is that land comes at a premium, and the surface on which power can be produced is fixed (S).

The first implication is that the drive toward more power pushes the design toward progressively larger sizes, ultimately toward a single power plant assigned to an area of order S. Progress in this direction is not always possible. From the point of view of producing useful power per unit area, one counterproductive aspect of a larger area served by a single power plant is that the access of all the flows (in, out) that serve the power plant and the inhabitants who depend on it is impeded when the area increases. Every stream that

flows has a flow rate that increases with S, and must overcome a resistance that increases in proportion with the distance that the stream travels, namely $S^{1/2}$.

For example, if the stream is the power generated by the solar plant, then the stream is proportional to ηS (or $S^{3/2}$), and the useful power destroyed in order to distribute the stream on S increases as $S^{3/2} \cdot S^{1/2} = S^2$. This means that the net power that is received by the population living on S has two components, one positive and the other negative

$$\dot{W}_{net} = aS^{3/2} - bS^2 \qquad (24)$$

where (a, b) are two constants fixed by the technology of the time. When the two components are in balance, the net power is maximum. This happens when the surface allocated to the single power plant has an optimal size,

$$S_0 \sim \left(\frac{a}{b}\right)^2 \qquad (25)$$

In this case $\dot{W}_{net,max}$ scales as a $S_0^{3/2}$, and the efficiency scales as $S_0^{1/2}$. A larger power plant on a larger surface would be more efficient and more productive, but it will be less efficient in its ability to distribute the power to its users on the area.

The second implication is that because the largest size of a single power plant is fixed by the technology tradeoff shown in Eq. (24), a larger territory $\left(X^2 >> S_0\right)$ must be covered with several power plants. Should X^2 be covered by a few large power plants, or by many small power plants? And, in what pattern, i.e. in what arrangement on the map?

To illustrate this second aspect of global design, consider the square territory designs shown in Fig. 2, where one disc area $(\pi/4)D_i^2$ plays the role of S_0 in the preceding discussion. Each disc of diameter D_i is the land area allocated to the power plant of size πR_i^2, as shown in the upper detail of Fig. 1. The size D_i scales with R_i, and $D_i >> R_i$. The power generated on the square territory by all the power plants is proportional to the sum:

$$\sum = n_0 D_0^3 + n_1 D_1^3 + n_2 D_2^3 + \ldots \qquad (26)$$

where $n_0, n_1, n_2, \ldots$ are the numbers of discs of sizes $D_0, D_1, D_2, \ldots$ that are inscribed in the area $X \times X$. The diameters D_i are cubed because of the earlier discussion, which showed that the power generated by one plant increases as $S_0^{3/2}$, i.e. as the length scale cubed. Because the territory X^2 is fixed, we may use X as length scale relative to which to nondimensionalize all the disc diameters,

$$\tilde{D}_i = D_i / X \qquad (27)$$

such that Eq. (26) becomes

$$\frac{\sum}{X^3} = n_0 \tilde{D}_0^3 + n_1 \tilde{D}_1^3 + n_2 \tilde{D}_2^3 + \ldots \qquad (28)$$

There is an infinite number of ways in which to fill the square with discs of many sizes, such that the largest has a diameter D_0 of order X [or of order $S_0^{1/2}$, cf. Eq. (25)]. In the design of Fig. 2a, the disc numbers and diameters are:

$$n_0 = 1 \quad \tilde{D}_0 = 1$$
$$n_1 = 1 \quad \tilde{D}_1 = 2^{1/2} - 1 = 0.414 \qquad (29$$
$$n_2 = 4 \quad \tilde{D}_2 = \left(1.5 - 2^{1/2}\right) / \left(1.5 - 2^{-1/2}\right) = 0.1(\quad)$$

The global performance of this design is indicated by

$$\frac{\Sigma_a}{X^3} = 1\cdot(1)^3 + 1\cdot\left(2^{1/2}-1\right)^3 + 4\cdot\left[\left(1.5-2^{1/2}\right)/\left(1.5-2^{-1/2}\right)\right]^3 + .. \cong 1.076 \quad (30)$$

If a disc pattern similar to Fig. 2a would be inscribed in a large circular area, as opposed to a square, and if the number of D_i scales would be infinite, the resulting pattern would be fractal: the Apollonian gasket, or Apollonian net (named after the Greek geometrist Apollonius of Perga (cca. 262 BC – 190 BC)).

Consider next a design where the largest power plants are more numerous, e.g. Fig. 2b. The downside of such a design is that when n_0 increases D_0 decreases. The design of Fig. 2b has the following numbers and sizes of power discs:

$$n_0 = 2 \qquad \tilde{D}_0 = 2^{-1/2} = 0.707$$
$$n_1 = 2 \qquad \tilde{D}_1 = 1 - 2^{-1/2} = 0.293$$
$$n_2 = 8 \qquad \tilde{D}_2 = \frac{3-2^{3/2}}{3\cdot 2^{1/2}-2} = 0.07 \quad (31)$$

The global power generation rate in Fig. 2b is

$$\frac{\Sigma_b}{X^3} = 2\cdot\left(2^{-1/2}\right)^3 + 2\cdot\left(1-2^{-1/2}\right)^3 + 8\cdot\left[\left(3-2^{3/2}\right)/\left(3\cdot 2^{1/2}-2\right)\right]^3 + \ldots \cong 0.761 \quad (32)$$

The power decreases by 29 percent in going from design (a) to design (b).

Another possible design is shown in Fig. 2c, where the plant sizes, numbers and global performance are as follows:

$$n_0 = 4 \qquad \tilde{D}_0 = 2^{-1} = 0.5$$
$$n_1 = 4 \qquad \tilde{D}_1 = 2^{-1/2} - 2^{-1} = 0.207$$
$$n_2 = 16 \qquad \tilde{D}_2 = \frac{3-2^{3/2}}{2\left(3-2^{1/2}\right)} = 0.054 \quad (33)$$

$$\frac{\Sigma_c}{X^3} = 4\cdot\left(2^{-1}\right)^3 + 4\cdot\left(2^{-1/2}-2^{-1}\right)^3 + 16\cdot\left[\left(3-2^{3/2}\right)/\left(6-2^{3/2}\right)\right]^3 + \ldots \cong 0.538 \quad (34)$$

(a)

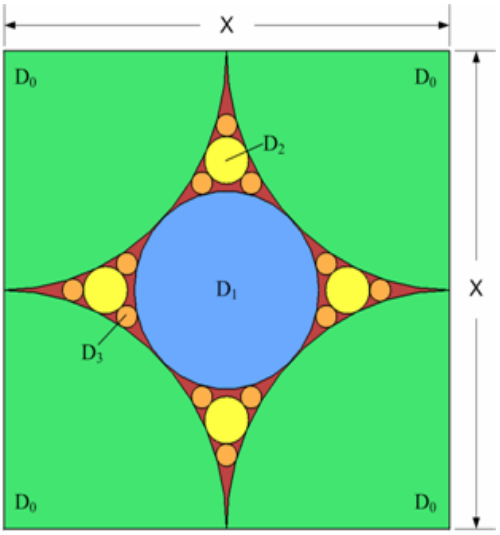

(b)

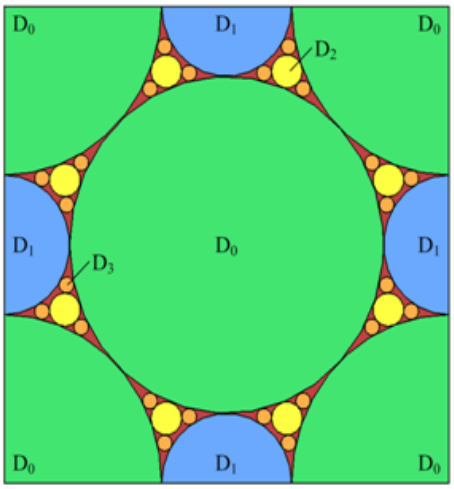

(c)

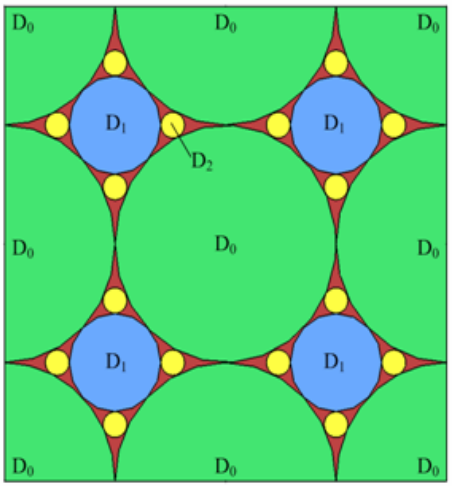

Figure 2

(d)

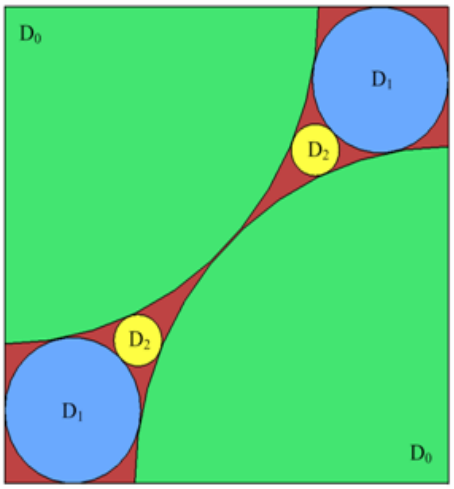

(e)

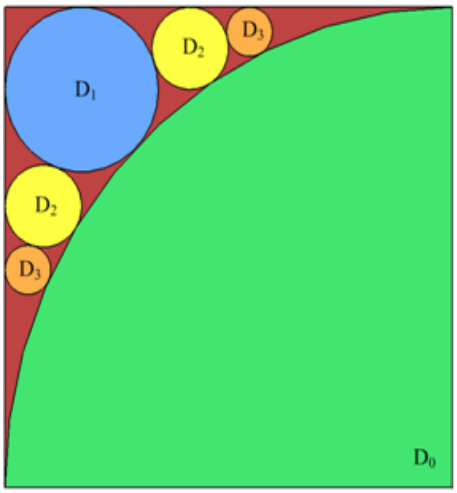

Figure 2 (Continued)

This power level is half of that of design (a). Note further that pattern (c) is the same as pattern (a), and that the length scale of the discs on (c) are half of the length scale on (a). In conclusion, if all the area elements shrink by a factor of $1/4$ (because all the D_i's shrink by $1/2$), then the aggregate power output of the $X \times X$ territory decreases by $1/2$.

The patterns in Figs. 2a–c are diagonally symmetric. In order to increase the D_0 scale, the pattern must be asymmetric, as in Figs. 2d and e. For the design of Fig. 2d we obtain

$$\begin{aligned} n_0 &= 1/2 \quad \tilde{D}_0 = 2^{1/2} = 1.414 \\ n_1 &= 2 \quad \tilde{D}_1 = 2 + 2^{1/2} - 2\cdot\left(1+2^{1/2}\right)^{1/2} \\ &\qquad = 0.307 \\ n_2 &= 2 \quad \tilde{D}_2 = 0.109 \end{aligned} \tag{35}$$

$$\frac{\sum_d}{X^3} \cong 1.475 \tag{36}$$

Here the power output is greater than in design (a). One reason is that the largest scale of design (d) (namely $D_{0,d}$) is 1.41 times larger than the D_0 scale in design (a). If we recalculate Eq. (36) by reducing all the D_i's by the factor $(1.41)^{-1} = 0.71$ and adding more discs to cover the whole land area (as shown in Fig. 3d), the value of $\sum_d / X^3$ becomes approximately 1.049. This is comparable with the performance of design (a).

The corresponding geometry and performance of the design of Fig. 2e are

$$\begin{aligned} n_0 &= 1/4 \quad \tilde{D}_0 = 2 \\ n_1 &= 1 \quad \tilde{D}_1 = 0.343 \\ n_2 &= 2 \quad \tilde{D}_2 = 0.172 \\ n_3 &= 2 \quad \tilde{D}_3 = 0.103 \end{aligned} \tag{37}$$

$$\frac{\sum_e}{X^3} \cong 2.061 \tag{38}$$

The large value of $\sum_e / X^3$ is due to the fact that the largest element ($D_{0,e}$) is larger than in all the preceding designs. On the other hand, if $D_{0,e}$ is reduced to the size of $D_{0,a}$, as illustrated in Fig. 3e, then the value of $\sum_e / X^3$ drops from 2.06 to 1.03.

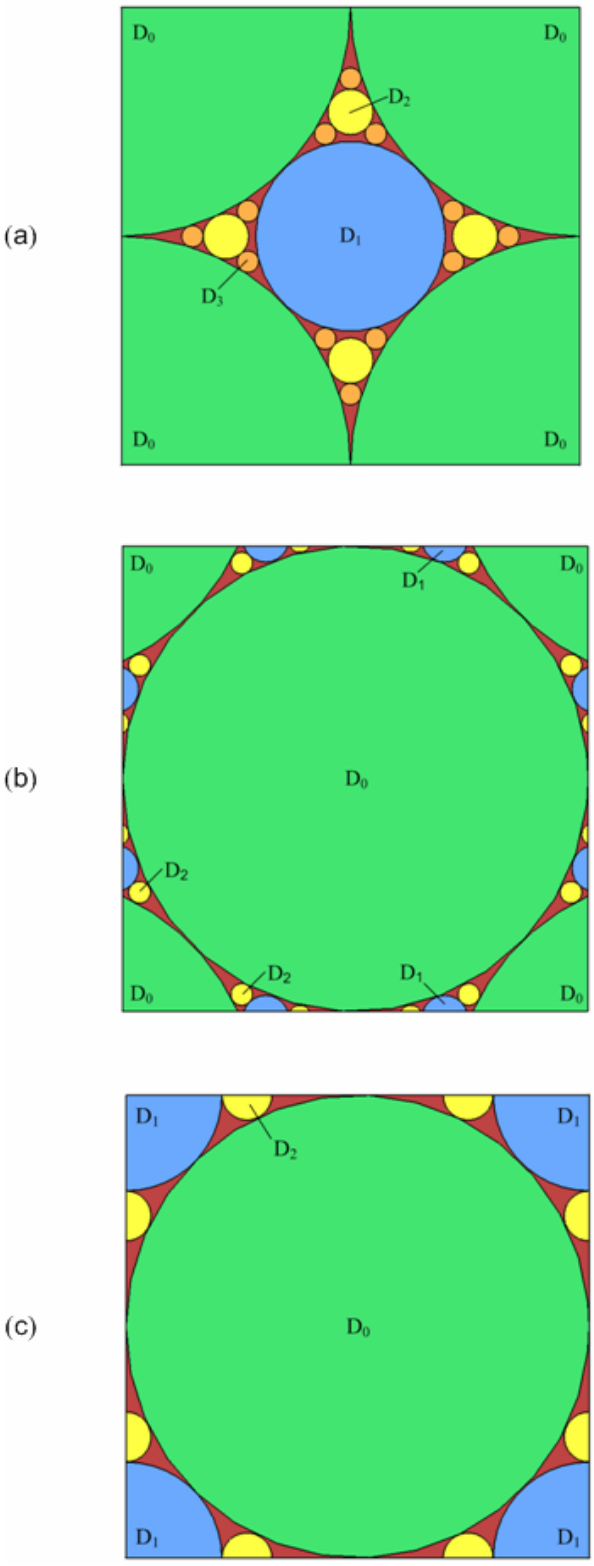

Figure 3

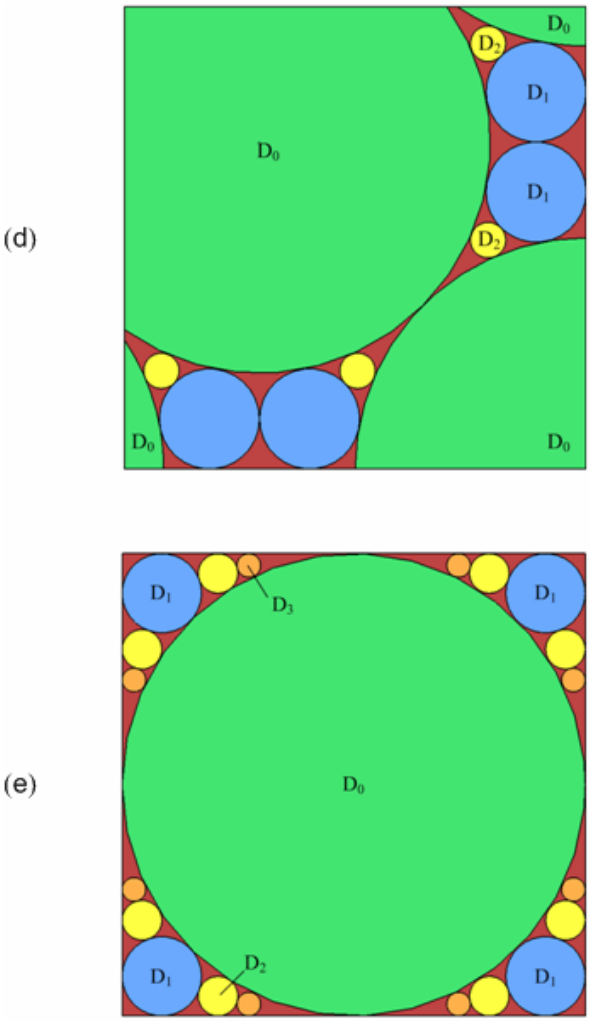

Figure 3 (Continued)

This calculation was performed for designs (b) and (c) as well, so that we may evaluate the five designs on the same basis: the same territory (X) and the same largest element (D_0). The new version of these designs is shown in Fig. 3, where Fig. 3a is identical to Fig. 2a, and Figs. 3b-e derive from Figs. 2b-e, respectively. The overall comparison is presented in Table 1. The highest performance is offered by design (b), in which n_0 is the largest when compared with other designs.

Table 1. The global power output of the multi-size arrangements (a) – (e) shown in Fig. 3

when the largest length scale (D_0) is the same in all the arrangements.

Design	$\sum/X^3$
a	1.076
b	1.199
c	1.076
d	1.049
e	1.025

5. Compactness

In conclusion, the power generated depends primarily on the land area occupied by the largest plant. To investigate this effect more closely, we define the dimensionless *compactness* :

$$C = \frac{\text{area covered by power plants}}{\text{land area}} \qquad (39)$$

or, specifically,

$$\begin{aligned} C_0 &= A_{D_0}/X^2 \\ C_{0,1} &= \left(A_{D_0} + A_{D_1}\right)/X^2 \\ C_{0,1,2} &= \left(A_{D_0} + A_{D_1} + A_{D_2}\right)/X^2 \end{aligned} \qquad (40)$$

Figure 4 shows the compactness of each of the patterns of Fig. 3, as a function of their corresponding dimensionless power output, $\sum/X^3$. In this comparison the largest length scale of the pattern (D_0) is the same in all five designs. Each curve in Fig. 4 is the result of curve-fitting the three points that correspond to the $C_0, C_{0,1}$ and $C_{0,1,2}$ values of each design.

It is evident from the results plotted in Fig. 4 that $\sum/X^3$ is a weak function of compactness. In other words, the global performance depends mainly on the land area that is being used. Again, the $\sum/X^3$ value in design b is greater than in other designs because it has the largest n_0. It should be noted that designs a, c, d and e have the same n_0, but the $\sum/X^3$ values of these designs are different.

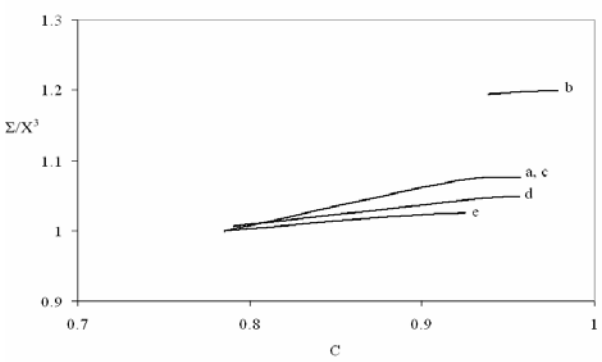

Figure 4

The performance depends on the D_1 value of each design. To conclude, the efficiency in power production of large plants is better than small plants, and an economy of scale emerges.

6. Conclusions

In this paper we determined the optimal configuration of solar chimney power plants, based on constructal theory. First, we found the relationship between maximum power and geometry, and demonstrated that the maximum flow power is a function of the length scale of the plant. Larger plants produce more power per unit of territory. Although a single large power plant occupies the whole area and generates most power, it is less efficient in distributing the power on the area. The power production can be designed by allocating optimally the land area to the plant.

We presented several arrangements for distributing the multi-scale plants on the square area: few large and many small, in the right arrangement. The most important factor in this design is the land area allocated to the largest plant. We also defined the dimensionless parameter called compactness, which is the ratio

between the area covered by power plants and the land area, and showed that the efficiency in power production also depends on the total land area that is being used.

Few large, or many small? The answer, which in this paper was illustrated for solar chimney power plants, is generally applicable to all proposals of power harvesting from land areas that possess low-density resources. Candidates are solar thermal and photovoltaic power installations, where the power is generated on round areas with solar collectors and central power plant, which resemble the unit shown in Fig. 1. For example, it is being contemplated to use large areas in the Sahara to collect, generate and distribute solar power [23]. How to use the land area most efficiently is the “few large, many small” principle proposed and explored in this paper.

7. Acknowledgement

This research was sponsored by the SUT Research and Development fund of Suranaree University of Technology (SUT). The work of Profs. Adrian Bejan and Sylvie Lorente was supported by a grant from the National Science Foundation.

8. References

[1] J. Schlaich (1995). The Solar Chimney. Edition Axel Menges: Stuttgart, Germany.

[2] N. Pasumarthi, S. A. Sherif (1998). Experimental and theoretical performance of a demonstration solar chimney model Part I: mathematical model development. International Journal of Energy Research, Vol. 22, pp.277–288.

[3] N. Pasumarthi, S. A. Sherif (1998). Experimental and theoretical performance of a demonstration solar chimney modelPart II: experimental and theoretical results and economic analysis. International Journal of Energy Research, Vol. 22, pp. 443–461.

[4] M. M. Padki, S. A. Sherif (1999). On a simple analytical model for solar chimneys. International Journal of Energy Research, Vol. 23(4), pp 345-349.

[5] M. A. K. Lodhi (1999). Application of helio-aero-gravity concept in producing energy and suppressing pollution. Energy Conversion and Management, Vol. 40(4), pp. 407–421.

[6] H. Pastohr, O. Kornadt, K. Gürlebeck (2004). Numerical and analytical calculations of the temperature and flow field in the upwind power plant. International Journal of Energy Research, Vol. 28(6), pp. 495-510.

[7] T. Ming, W. Liu, G. Xu (2006). Analytical and numerical investigation of the solar chimney power plant systems. International Journal of Energy Research, Vol. 30, pp. 861-873.

[8] T. Ming, W. Liu, Y. Pan, G. Xu (2008). Numerical analysis of flow and heat transfer characteristics in solar chimney power plants with energy storage layer. Energy Conversion and Management, Vol. 49(2008), pp. 2872-2879.

[9] B.A. Kashiwa, B.C. Kashiwa (2008). The solar cyclone: A solar chimney for harvesting atmospheric water. Energy, Vol. 33(2), pp. 331-339.

[10] S. Nizetic, N. Ninic, B. Klarin (2008). Analysis and feasibility of implementing solar chimney power plants in the Mediterranean region. Energy, Vol. 33(2008), pp.1680–1690.

[11] X. Zhou, J. Yang, J. Wang, B. Xiao (2009). Novel concept for producing energy

integrating a solar collector with a man made mountain hollow. Conversion and Management, Vol. 50(2009), pp. 478-854.

[12] Y. J. Dai, H. B. Huang, R. Z. Wang (2003). Case study of solar chimney power plants in northwestern regions of China. Renewable Energy, Vol. 28, pp. 1295-1304.

[13] E. Bilgen, J. Rheault (2005). Solar chimney power plants for high latitudes. Solar Energy, Vol. 79, pp. 449-458.

[14] A. J. Gannon, T. W. Von Backström (2000). Solar chimney cycle analysis with system loss and solar collector performance. Journal of Solar Energy Engineering, Vol. 122. pp. 133-137.

[15] T. W. Von Backström (2003). Calculation of pressure and density in solar power plant chimneys. Journal of Solar Energy Engineering, Vol. 125, pp 127-129.

[16] J. P. Pretorius, D. G. Kröger (2006). Critical evaluation of solar chimney power plant performance. Solar Energy, Vol. 80, pp. 535-544.

[17] J. P. Pretorius, D. G. Kröger (2006). Solar chimney power plant performance. Journal of Solar Energy Engineering, Vol. 128, pp. 302-311.

[18] M. A. S. Bernardes, T. W. Von Backström, D. G. Kröger (2009). Analysis of some available heat transfer coefficients applicable to solar chimney power plant collectors. Solar Energy, Vol. 83, pp. 264-275.

[19] A. Bejan, S. Lorente (2008). Design with Constructal Theory, Wiley, Hoboken, NJ.

[20] A. Bejan (2004). Convection Heat Transfer, 3rd ed., Wiley, Hoboken, NJ.

[21] T. Chitsomboon (2001). A validated analytical model for flow in solar chimney. International Journal of Renewable Energy Engineering, Vol. 3 (2001), pp. 339-346.

[22] Y. S. Kim, S. Lorente, A. Bejan (2009). Distribution of size in steam turbine power plants. International Journal of Energy Research, doi: 10.1002/er.1528.

[23] H. Liebs (2009). Fantasme technologique au Sahara. Courrier International, No. 981, 20 August 2009, pp. 48-49.

Nomenclature

a, b	constants
A	total surface of the chimney and the roof, m^2
A_c	cross-sectional area, m^2
A_r	roof area, m^2
C	compactness
$C_{1,2,3,4}$	constants
c_P	specific heat at constant pressure, $J/kg\,K$
D	tower diameter, m, Fig. 1
$\tilde{D}$	dimensionless diameter
D_i	disc diameters, m
f	friction factor
g	gravitational acceleration, m/s^2
H	tower height, m, Fig. 1
h	roof height, m, Fig. 1
M	Mach number
$\dot{m}$	mass flow rate, kg/s
n_i	disc number
q''	solar heat flux, W/m^2
R	roof radius, m, Fig. 1
R_i	disc radii, m
S	territory, m^2
T_0	atmospheric temperature, K

U	velocity, m/s
$\dot{W}$	flow power, W
X	side of square territory, m^2

Greek symbols

β	volumetric coefficient of thermal expansion, 1/K
ΔP	pressure drop, Pa
ΔP_{acc}	acceleration pressure drop, Pa
ΔT	temperature difference in roof portion, K
η	efficiency
λ	Lagrange multiplier
ρ	density, kg/m^3
ρ_0	air density at T_0, kg/m^3
$\sum$	quantity proportional to the total power generation rate
τ	fluid shear stress
Ψ	auxiliary function, Eq. (20)

Subscripts

max	maximum
o	optimal
net	net
w	wall
x	horizontal passage
y	vertical passage
1	roof inlet
2	roof outlet